4 Leptonic and semileptonic kaon and pion decay and $|V_{ud}|$ and $|V_{us}|$

This section summarizes state-of-the-art lattice calculations of the leptonic kaon and pion decay constants and the kaon semileptonic-decay form factor and provides an analysis in view of the Standard Model. With respect to the previous edition of the FLAG review [1] the data in this section has been updated. As in Ref. [1], when combining lattice data with experimental results, we take into account the strong $SU(2)$ isospin correction, either obtained in lattice calculations or estimated by using chiral perturbation theory, both for the kaon leptonic decay constant $f_{K^\pm}$ and for the ratio $f_{K^\pm}/f_{\pi^\pm}$.

4.1 Experimental information concerning $|V_{ud}|$, $|V_{us}|$, $f_+(0)$ and $f_{K^\pm}/f_{\pi^\pm}$

The following review relies on the fact that precision experimental data on kaon decays very accurately determine the product $|V_{us}|f_+(0)$ [2] and the ratio $|V_{us}/V_{ud}|f_{K^\pm}/f_{\pi^\pm}$ [2, 3]:

$$|V_{us}|f_+(0) = 0.2165(4)\,, \qquad \left|\frac{V_{us}}{V_{ud}}\right| \frac{f_{K^\pm}}{f_{\pi^\pm}} = 0.2760(4)\,. \tag{54}$$

Here and in the following $f_{K^\pm}$ and $f_{\pi^\pm}$ are the isospin-broken decay constants, respectively, in QCD (the electromagnetic effects have already been subtracted in the experimental analysis using chiral perturbation theory). We will refer to the decay constants in the $SU(2)$ isospin-symmetric limit as f_K and f_π (the latter at leading order in the mass difference $(m_u - m_d)$ coincides with $f_{\pi^\pm}$). $|V_{ud}|$ and $|V_{us}|$ are elements of the Cabibbo-Kobayashi-Maskawa matrix and $f_+(t)$ represents one of the form factors relevant for the semileptonic decay $K^0 \to \pi^-\ell\,\nu$, which depends on the momentum transfer t between the two mesons. What matters here is the value at $t = 0$: $f_+(0) \equiv f_+^{K^0\pi^-}(t)\big|_{t\to 0}$. The pion and kaon decay constants are defined by[1]

$$\langle 0|\,\bar{d}\gamma_\mu\gamma_5\,u|\pi^+(p)\rangle = i\,p_\mu f_{\pi^+}\,, \qquad \langle 0|\,\bar{s}\gamma_\mu\gamma_5\,u|K^+(p)\rangle = i\,p_\mu f_{K^+}\,.$$

In this normalization, $f_{\pi^\pm} \simeq 130$ MeV, $f_{K^\pm} \simeq 155$ MeV.

The measurement of $|V_{ud}|$ based on superallowed nuclear β transitions has now become remarkably precise. The result of the update of Hardy and Towner [9], which is based on 20 different superallowed transitions, reads[2]

$$|V_{ud}| = 0.97417(21)\,. \tag{55}$$

The matrix element $|V_{us}|$ can be determined from semiinclusive τ decays [16–19]. Separating the inclusive decay $\tau \to$ hadrons $+\,\nu$ into nonstrange and strange final states, e.g. HFAG 14 [20] obtain

$$|V_{us}| = 0.2176(21)\,. \tag{56}$$

[1] The pion decay constant represents a QCD matrix element – in the full Standard Model, the one-pion state is not a meaningful notion: the correlation function of the charged axial current does not have a pole at $p^2 = M_{\pi^+}^2$, but a branch cut extending from $M_{\pi^+}^2$ to ∞. The analytic properties of the correlation function and the problems encountered in the determination of f_π are thoroughly discussed in Ref. [4]. The "experimental" value of f_π depends on the convention used when splitting the sum $\mathcal{L}_{\rm QCD} + \mathcal{L}_{\rm QED}$ into two parts (compare Sec. 3.1.1). The lattice determinations of f_π do not yet reach the accuracy where this is of significance, but at the precision claimed by the Particle Data Group [3, 5], the numerical value does depend on the convention used [4, 6–8].

[2] It is not a trivial matter to perform the data analysis at this precision. In particular, isospin-breaking effects need to be properly accounted for [10–15]. For a review of recent work on this issue, we refer to Ref. [9].

Maltman et al. [18, 21, 22] and Gamiz et al. [23, 24] arrive at very similar values.

Inclusive hadronic τ decay offers an interesting way to measure $|V_{us}|$, but a number of open issues yet remain to be clarified. In particular, the value of $|V_{us}|$ as determined from τ decays differs from the result one obtains from assuming three-flavour SM-unitarity by more than three standard deviations [20]. It is important to understand this apparent tension better. A possibility is that at the current level of precision the treatment of higher orders in the operator product expansion and violations of quark-hadron duality may play a role. Very recently [25] a new implementation of the relevant sum rules has been elaborated suggesting a much larger value of $|V_{us}|$ with respect to the result (56), namely $|V_{us}| = 0.2228(23)$, which is in much better agreement with CKM unitarity. Another possibility is that τ decay involves new physics, but more work both on the theoretical and experimental side is required.

The experimental results in Eq. (54) are for the semileptonic decay of a neutral kaon into a negatively charged pion and the charged pion and kaon leptonic decays, respectively, in QCD. In the case of the semileptonic decays the corrections for strong and electromagnetic isospin breaking in chiral perturbation theory at NLO have allowed for averaging the different experimentally measured isospin channels [26]. This is quite a convenient procedure as long as lattice QCD does not include strong or QED isospin-breaking effects. Lattice results for f_K/f_π are typically quoted for QCD with (squared) pion and kaon masses of $M_\pi^2 = M_{\pi^0}^2$ and $M_K^2 = \frac{1}{2}\left(M_{K^\pm}^2 + M_{K^0}^2 - M_{\pi^\pm}^2 + M_{\pi^0}^2\right)$ for which the leading strong and electromagnetic isospin violations cancel. While progress is being made for including strong and electromagnetic isospin breaking in the simulations (e.g. Ref. [27–33]), for now contact to experimental results is made by correcting leading $SU(2)$ isospin breaking guided either by chiral perturbation theory or by lattice calculations.

4.2 Lattice results for $f_+(0)$ and $f_{K^\pm}/f_{\pi^\pm}$

The traditional way of determining $|V_{us}|$ relies on using estimates for the value of $f_+(0)$, invoking the Ademollo-Gatto theorem [50]. Since this theorem only holds to leading order of the expansion in powers of m_u, m_d and m_s, theoretical models are used to estimate the corrections. Lattice methods have now reached the stage where quantities like $f_+(0)$ or f_K/f_π can be determined to good accuracy. As a consequence, the uncertainties inherent in the theoretical estimates for the higher order effects in the value of $f_+(0)$ do not represent a limiting factor any more and we shall therefore not invoke those estimates. Also, we will use the experimental results based on nuclear β decay and τ decay exclusively for comparison – the main aim of the present review is to assess the information gathered with lattice methods and to use it for testing the consistency of the SM and its potential to provide constraints for its extensions.

The database underlying the present review of the semileptonic form factor and the ratio of decay constants is listed in Tabs. 13 and 14. The properties of the lattice data play a crucial role for the conclusions to be drawn from these results: range of M_π, size of LM_π, continuum extrapolation, extrapolation in the quark masses, finite-size effects, etc. The key features of the various data sets are characterized by means of the colour code specified in Sec. 2.1. More detailed information on individual computations are compiled in appendix B.2.

The quantity $f_+(0)$ represents a matrix element of a strangeness-changing null-plane charge, $f_+(0) = \langle K|Q^{us}|\pi\rangle$. The vector charges obey the commutation relations of the Lie algebra of $SU(3)$, in particular $[Q^{us}, Q^{su}] = Q^{uu-ss}$. This relation implies the sum rule $\sum_n |\langle K|Q^{us}|n\rangle|^2 - \sum_n |\langle K|Q^{su}|n\rangle|^2 = 1$. Since the contribution from the one-pion intermedi-

Collaboration	Ref.	N_f	publication status	chiral extrapolation	continuum extrapolation	finite-volume errors	$f_+(0)$
ETM 16	[34]	2+1+1	A	○	★	○	0.9709(45)(9)
FNAL/MILC 13E	[35]	2+1+1	A	★	★	★	0.9704(24)(22)
FNAL/MILC 13C	[36]	2+1+1	C	★	★	★	0.9704(24)(32)
JLQCD 16	[37]	2+1	C	○	■	★	$0.9636(36)(^{+50}_{-54})$
RBC/UKQCD 15A	[38]	2+1	A	★	○	○	0.9685(34)(14)
RBC/UKQCD 13	[39]	2+1	A	★	○	○	$0.9670(20)(^{+18}_{-46})$
FNAL/MILC 12I	[40]	2+1	A	○	○	★	0.9667(23)(33)
JLQCD 12	[41]	2+1	C	○	■	★	0.959(6)(5)
JLQCD 11	[42]	2+1	C	○	■	★	0.964(6)
RBC/UKQCD 10	[43]	2+1	A	○	■	★	$0.9599(34)(^{+31}_{-47})(14)$
RBC/UKQCD 07	[44]	2+1	A	○	■	★	0.9644(33)(34)(14)
ETM 10D	[45]	2	C	○	★	○	$0.9544(68)_{stat}$
ETM 09A	[46]	2	A	○	○	○	0.9560(57)(62)
QCDSF 07	[47]	2	C	■	■	★	$0.9647(15)_{stat}$
RBC 06	[48]	2	A	■	■	★	0.968(9)(6)
JLQCD 05	[49]	2	C	■	■	★	0.967(6), 0.952(6)

Table 13: Colour code for the data on $f_+(0)$.

ate state to the first sum is given by $f_+(0)^2$, the relation amounts to an exact representation for this quantity [51]:

$$f_+(0)^2 = 1 - \sum_{n\neq\pi} |\langle K|Q^{us}|n\rangle|^2 + \sum_n |\langle K|Q^{su}|n\rangle|^2 \,. \tag{57}$$

While the first sum on the right extends over nonstrange intermediate states, the second runs over exotic states with strangeness ± 2 and is expected to be small compared to the first.

The expansion of $f_+(0)$ in $SU(3)$ chiral perturbation theory in powers of m_u, m_d and m_s starts with $f_+(0) = 1 + f_2 + f_4 + \ldots$ [52]. Since all of the low-energy constants occurring in f_2 can be expressed in terms of M_π, M_K, M_η and f_π [53], the NLO correction is known. In the language of the sum rule (57), f_2 stems from nonstrange intermediate states with three mesons. Like all other nonexotic intermediate states, it lowers the value of $f_+(0)$: $f_2 = -0.023$ when using the experimental value of f_π as input. The corresponding expressions have also been derived in quenched or partially quenched (staggered) chiral perturbation theory [40, 54]. At the same order in the $SU(2)$ expansion [55], $f_+(0)$ is parameterized in terms of M_π and two *a priori* unknown parameters. The latter can be determined from the dependence of the lattice results on the masses of the quarks. Note that any calculation that relies on the χPT formula for f_2 is subject to the uncertainties inherent in NLO results: instead of using the physical value of the pion decay constant f_π, one may, for instance, work with the constant f_0 that occurs in the effective Lagrangian and represents the value of f_π in the chiral limit.

Although trading f_π for f_0 in the expression for the NLO term affects the result only at NNLO, it may make a significant numerical difference in calculations where the latter are not explicitly accounted for (the lattice results concerning the value of the ratio f_π/f_0 are reviewed in Sec. 5.3).

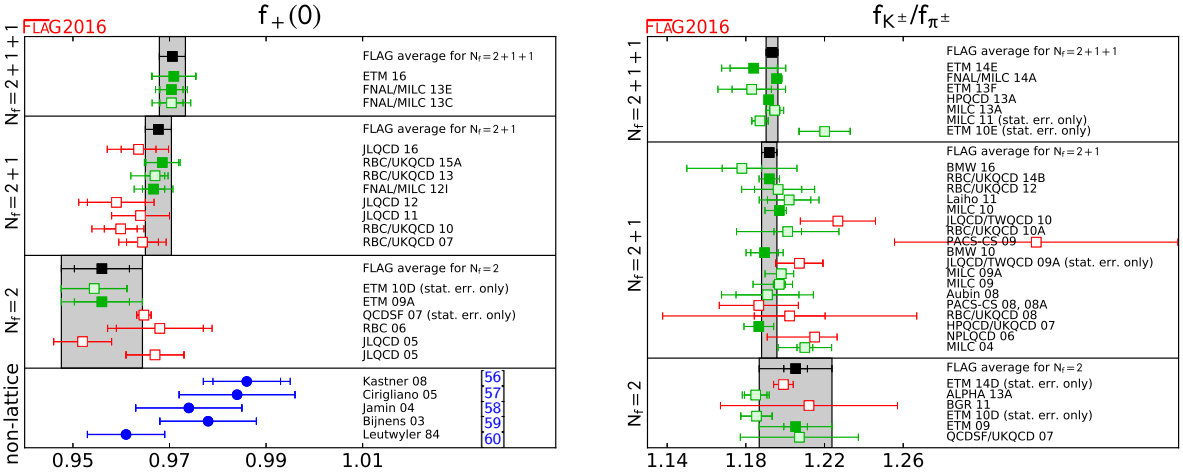

Figure 7: Comparison of lattice results (squares) for $f_+(0)$ and $f_{K^\pm}/f_{\pi^\pm}$ with various model estimates based on χPT (blue circles). The ratio $f_{K^\pm}/f_{\pi^\pm}$ is obtained in pure QCD including the $SU(2)$ isospin-breaking correction (see Sec. 4.3). The black squares and grey bands indicate our estimates. The significance of the colours is explained in Sec. 2.

The lattice results shown in the left panel of Fig. 7 indicate that the higher order contributions $\Delta f \equiv f_+(0) - 1 - f_2$ are negative and thus amplify the effect generated by f_2. This confirms the expectation that the exotic contributions are small. The entries in the lower part of the left panel represent various model estimates for f_4. In Ref. [60] the symmetry-breaking effects are estimated in the framework of the quark model. The more recent calculations are more sophisticated, as they make use of the known explicit expression for the $K_{\ell 3}$ form factors to NNLO in χPT [59, 61]. The corresponding formula for f_4 accounts for the chiral logarithms occurring at NNLO and is not subject to the ambiguity mentioned above.[3] The numerical result, however, depends on the model used to estimate the low-energy constants occurring in f_4 [56–59]. The figure indicates that the most recent numbers obtained in this way correspond to a positive or an almost vanishing rather than a negative value for Δf. We note that FNAL/MILC 12I [40] have made an attempt at determining a combination of some of the low-energy constants appearing in f_4 from lattice data.

4.3 Direct determination of $f_+(0)$ and $f_{K^\pm}/f_{\pi^\pm}$

All lattice results for the form factor $f_+(0)$ and many available results for the ratio of decay constants, that we summarize here in Tabs. 13 and 14, respectively, have been computed in isospin-symmetric QCD. The reason for this unphysical parameter choice is that there are only few simulations of $SU(2)$ isospin-breaking effects in lattice QCD, which is ultimately the cleanest way for predicting these effects [28, 31–33, 62–65]. In the meantime one relies

[3] Fortran programs for the numerical evaluation of the form factor representation in Ref. [59] are available on request from Johan Bijnens.

either on chiral perturbation theory [52, 66] to estimate the correction to the isospin limit or one calculates the breaking at leading order in $(m_u - m_d)$ in the valence quark sector by extrapolating the lattice data for the charged kaons to the physical value of the *up*(*down*)-quark mass (the result for the pion decay constant is always extrapolated to the value of the average light-quark mass $\hat{m}$). This defines the prediction for $f_{K^\pm}/f_{\pi^\pm}$.

Since the majority of the collaborations present their newest results including the strong $SU(2)$ isospin-breaking correction (as we will see this comprises the majority of results which qualify for inclusion into the FLAG average), we prefer to provide in Fig. 7 the overview of the world data of $f_{K^\pm}/f_{\pi^\pm}$, at variance with the choice made in the previous edition of the FLAG review [1]. For all the results of Tab. 14 provided only in the isospin-symmetric limit we apply individually an isospin correction which will be described later on (see equations Eqs. (62-63)).

The plots in Fig. 7 illustrate our compilation of data for $f_+(0)$ and $f_{K^\pm}/f_{\pi^\pm}$. The lattice data for the latter quantity are largely consistent even when comparing simulations with different N_f, while in the case of $f_+(0)$ a slight tendency to get higher values for increasing N_f seems to be visible, even if it does not exceed one standard deviation. We now proceed to form the corresponding averages, separately for the data with $N_f = 2+1+1$, $N_f = 2+1$ and $N_f = 2$ dynamical flavours and in the following we will refer to these averages as the "direct" determinations.

For $f_+(0)$ there are currently two computational strategies: FNAL/MILC uses the Ward identity to relate the $K \to \pi$ form factor at zero momentum transfer to the matrix element $\langle \pi|S|K\rangle$ of the flavour-changing scalar current. Peculiarities of the staggered fermion discretization used by FNAL/MILC (see Ref. [40]) makes this the favoured choice. The other collaborations are instead computing the vector current matrix element $\langle \pi|V_\mu|K\rangle$. Apart from FNAL/MILC 13C and the recent FNAL/MILC 13E all simulations in Tab. 13 involve unphysically heavy quarks and therefore the lattice data needs to be extrapolated to the physical pion and kaon masses corresponding to the $K^0 \to \pi^-$ channel. We note also that the recent computations of $f_+(0)$ obtained by the FNAL/MILC and RBC/UKQCD collaborations make use of the partially-twisted boundary conditions to determine the form-factor results directly at the relevant kinematical point $q^2 = 0$ [97, 98], avoiding in this way any uncertainty due to the momentum dependence of the vector and/or scalar form factors. The ETM collaboration uses partially-twisted boundary conditions to compare the momentum dependence of the scalar and vector form factors with the one of the experimental data [34, 45], while keeping at the same time the advantage of the high-precision determination of the scalar form factor at the kinematical end-point $q^2_{max} = (M_K - M_\pi)^2$ [46, 99] for the interpolation at $q^2 = 0$.

According to the colour codes reported in Tab. 13 and to the FLAG rules of Sec. 2.2, only the result ETM 09A with $N_f = 2$, the results FNAL/MILC 12I and RBC/UKQCD 15A with $N_f = 2+1$ and the results FNAL/MILC 13E and ETM 16 with $N_f = 2+1+1$ dynamical flavours of fermions, respectively, can enter the FLAG averages.

At $N_f = 2{+}1{+}1$ the new result from the FNAL/MILC collaboration, $f_+(0) = 0.9704(24)(22)$ (FNAL/MILC 13E), is based on the use of the Highly Improved Staggered Quark (HISQ) action (for both valence and sea quarks), which has been taylored to reduce staggered taste-breaking effects, and includes simulations with three lattice spacings and physical light-quark masses. These features allow to keep the uncertainties due to the chiral extrapolation and to the discretization artifacts well below the statistical error. The remaining largest systematic uncertainty comes from finite-size effects.

The new result from the ETM collaboration, $f_+(0) = 0.9709(45)(9)$ (ETM 16), makes

Collaboration	Ref.	N_f	publication status	chiral extrapolation	continuum extrapolation	finite-volume errors	f_K/f_π	$f_{K^\pm}/f_{\pi^\pm}$
ETM 14E	[67]	2+1+1	A	○	★	○	1.188(11)(11)	1.184(12)(11)
FNAL/MILC 14A	[68]	2+1+1	A	★	★	★		$1.1956(10)(^{+26}_{-18})$
ETM 13F	[69]	2+1+1	C	○	★	○	1.193(13)(10)	1.183(14)(10)
HPQCD 13A	[70]	2+1+1	A	★	○	★	1.1948(15)(18)	1.1916(15)(16)
MILC 13A	[71]	2+1+1	A	★	★	★		1.1947(26)(37)
MILC 11	[72]	2+1+1	C	○	○	○		$1.1872(42)^{\dagger}_{\text{stat.}}$
ETM 10E	[73]	2+1+1	C	○	○	○	$1.224(13)_{\text{stat}}$	
BMW 16	[74, 75]	2+1	P	★	★	★	1.182(10)(26)	
RBC/UKQCD 14B	[76]	2+1	A	★	★	★	1.1945(45)	
RBC/UKQCD 12	[77]	2+1	A	★	○	★	1.199(12)(14)	
Laiho 11	[78]	2+1	C	○	★	○		$1.202(11)(9)(2)(5)^{\dagger\dagger}$
MILC 10	[79]	2+1	C	○	★	★		$1.197(2)(^{+3}_{-7})$
JLQCD/TWQCD 10	[80]	2+1	C	○	■	★	1.230(19)	
RBC/UKQCD 10A	[81]	2+1	A	○	○	★	1.204(7)(25)	
PACS-CS 09	[82]	2+1	A	★	■	■	1.333(72)	
BMW 10	[83]	2+1	A	★	★	★	1.192(7)(6)	
JLQCD/TWQCD 09A	[84]	2+1	C	○	■	■	$1.210(12)_{\text{stat}}$	
MILC 09A	[85]	2+1	C	○	★	★		$1.198(2)(^{+6}_{-8})$
MILC 09	[86]	2+1	A	○	★	★		$1.197(3)(^{+6}_{-13})$
Aubin 08	[87]	2+1	C	○	○	○		1.191(16)(17)
PACS-CS 08, 08A	[27, 88]	2+1	A	★	■	■	1.189(20)	
RBC/UKQCD 08	[89]	2+1	A	○	■	★	1.205(18)(62)	
HPQCD/UKQCD 07	[90]	2+1	A	○	○	○	1.189(2)(7)	
NPLQCD 06	[91]	2+1	A	○	■	■	$1.218(2)(^{+11}_{-24})$	
MILC 04	[66]	2+1	A	○	○	○		1.210(4)(13)
ETM 14D	[92]	2	C	★	■	○	$1.203(5)_{\text{stat}}$	
ALPHA 13A	[93]	2	C	★	★	★	1.1874(57)(30)	
BGR 11	[94]	2	A	○	■	■	1.215(41)	
ETM 10D	[45]	2	C	○	★	○	$1.190(8)_{\text{stat}}$	
ETM 09	[95]	2	A	○	★	○	1.210(6)(15)(9)	
QCDSF/UKQCD 07	[96]	2	C	○	○	★	1.21(3)	

† Result with statistical error only from polynomial interpolation to the physical point.
†† This work is the continuation of Aubin 08.

Table 14: Colour code for the data on the ratio of decay constants: f_K/f_π is the pure QCD $SU(2)$-symmetric ratio, while $f_{K^\pm}/f_{\pi^\pm}$ is in pure QCD including the $SU(2)$ isospin-breaking correction.

use of the twisted-mass discretization adopting three values of the lattice spacing in the range $0.06 - 0.09$ fm and and pion masses simulated in the range $210 - 450$ MeV. The chiral and continuum extrapolations are performed in a combined fit together with the momentum

dependence, using both a $SU(2)$-χPT inspired Ansatz (following Ref. [45]) and a modified z-expansion fit. The uncertainties coming from the chiral extrapolation, the continuum extrapolation and the finite-volume effects turn out to be well below the dominant statistical error, which includes also the error due to the fitting procedure. A set of synthetic data points, representing both the vector and the scalar semileptonic form factors at the physical point for several selected values of q^2, is provided together with the corresponding correlation matrix.

At $N_f = 2 + 1$ there is a new result from the RBC/UKQCD collaboration, $f_+(0) = 0.9685(34)(14)$ [38] (RBC/UKQCD 15A), which satisfies all FLAG criteria for entering the average. RBC/UKQCD 15A superseeds RBC/UKQCD 13 thanks to two new simulations at the physical point. The other result eligible to enter the FLAG average at $N_f = 2+1$ is the one from FNAL/MILC 12I, $f_+(0) = 0.9667(23)(33)$. The two results, based on different fermion discretizations (staggered fermions in the case of FNAL/MILC and domain wall fermions in the case of RBC/UKQCD) are in nice agreement. Moreover, in the case of FNAL/MILC the form factor has been determined from the scalar current matrix element, while in the case of RBC/UKQCD it has been determined including also the matrix element of the vector current. To a certain extent both simulations are expected to be affected by different systematic effects.

RBC/UKQCD 15A has analyzed results on ensembles with pion masses down to 140 MeV, mapping out the complete range from the $SU(3)$-symmetric limit to the physical point. No significant cut-off effects (results for two lattice spacings) were observed in the simulation results. Ensembles with unphysical light-quark masses are weighted to work as a guide for small corrections toward the physical point, reducing in this way the model dependence in the fitting ansatz. The systematic uncertainty turns out to be dominated by finite-volume effects, for which an estimate based on effective theory arguments is provided.

The result FNAL/MILC 12I is from simulations reaching down to a lightest RMS pion mass of about 380 MeV (the lightest valence pion mass for one of their ensembles is about 260 MeV). Their combined chiral and continuum extrapolation (results for two lattice spacings) is based on NLO staggered chiral perturbation theory supplemented by the continuum NNLO expression [59] and a phenomenological parameterization of the breaking of the Ademollo-Gatto theorem at finite lattice spacing inherent in their approach. The p^4 low-energy constants entering the NNLO expression have been fixed in terms of external input [100].

The ETM collaboration uses the twisted-mass discretization and provides at $N_f = 2$ a comprehensive study of the systematics [45, 46], by presenting results for four lattice spacings and by simulating at light pion masses (down to $M_\pi = 260$ MeV). This makes it possible to constrain the chiral extrapolation, using both $SU(3)$ [53] and $SU(2)$ [55] chiral perturbation theory. Moreover, a rough estimate for the size of the effects due to quenching the strange quark is given, based on the comparison of the result for $N_f = 2$ dynamical quark flavours [95] with the one in the quenched approximation, obtained earlier by the SPQcdR collaboration [99].

We now compute the $N_f = 2+1+1$ FLAG-average for $f_+(0)$ using the FNAL/MILC 13E and ETM 16 (uncorrelated) results, the $N_f = 2 + 1$ FLAG-average based on FNAL/MILC 12I and RBC/UKQCD 15A, which we consider uncorrelated, while for $N_f = 2$ we consider

directly the ETM 09A result, respectively:

$$\text{direct, } N_f = 2+1+1: \qquad f_+(0) = 0.9706(27) \qquad \text{Ref. [34, 35]}, \tag{58}$$

$$\text{direct, } N_f = 2+1: \qquad f_+(0) = 0.9677(27) \qquad \text{Refs. [38, 40]}, \tag{59}$$

$$\text{direct, } N_f = 2: \qquad f_+(0) = 0.9560(57)(62) \qquad \text{Ref. [46]}, \tag{60}$$

where the brackets in the third line indicate the statistical and systematic errors, respectively. We stress that the results (58) and (59), corresponding to $N_f = 2+1+1$ and $N_f = 2+1$ respectively, include already simulations with physical light-quark masses.

In the case of the ratio of decay constants the data sets that meet the criteria formulated in the introduction are HPQCD 13A [70], FNAL/MILC 14A [68] (which updates MILC 13A [71]) and ETM 14E [67] with $N_f = 2+1+1$, MILC 10 [79], BMW 10 [83], HPQCD/UKQCD 07 [90] and RBC/UKQCD 12 [77] (which is an update of RBC/UKQCD 10A [81]) with $N_f = 2+1$ and ETM 09 [95] with $N_f = 2$ dynamical flavours.

ETM 14E uses the twisted-mass discretization and provides a comprehensive study of the systematics by presenting results for three lattice spacings in the range $0.06 - 0.09$ fm and and for pion masses in the range $210 - 450$ MeV. This makes it possible to constrain the chiral extrapolation, using both $SU(2)$ [55] chiral perturbation theory and polynomial fits. The ETM collaboration always includes the spread in the central values obtained from different ansätze into the systematic errors. The final result of their analysis is $f_{K^\pm}/f_{\pi^\pm} = 1.184(12)_{\text{stat+fit}}(3)_{\text{Chiral}}(9)_{\text{a}^2}(1)_{Z_P}(3)_{FV}(3)_{IB}$ where the errors are (statistical + the error due to the fitting procedure), due to the chiral extrapolation, the continuum extrapolation, the mass-renormalization constant, the finite-volume and (strong) isospin-breaking effects.

FNAL/MILC 14A has determined the ratio of the decay constants from a comprehensive set of HISQ ensembles with $N_f = 2+1+1$ dynamical flavours. They have generated ensembles for four values of the lattice spacing ($0.06 - 0.15$ fm, scale set with f_{π^+}) and with both physical and unphysical values of the light sea-quark masses, controlling in this way the systematic uncertainties due to chiral and continuum extrapolations. With respect to MILC 13A they have increased the statistics and added an important ensemble at the finest lattice spacing and for physical values of the light-quark mass. The final result of their analysis is $f_{K^\pm}/f_{\pi^\pm} = 1.1956(10)_{\text{stat}}(^{+23}_{-14})_{\text{a}^2}(10)_{FV}(5)_{EM}$ where the errors are statistical, due to the continuum extrapolation, finite-volume and electromagnetic effects. With respect to MILC 13A a factor of $\simeq 2.6$, 1.8 and $\simeq 1.7$ has been gained for the statistical, the discretization and the finite-volume errors.

HPQCD 13A analyzes ensembles generated by MILC and therefore its study of $f_{K^\pm}/f_{\pi^\pm}$ is based on the same set of ensembles bar the one for the finest lattice spacing ($a = 0.09 - 0.15$ fm, scale set with f_{π^+} and relative scale set with the Wilson flow [101, 102]) supplemented by some simulation points with heavier quark masses. HPQCD employs a global fit based on continuum NLO $SU(3)$ chiral perturbation theory for the decay constants supplemented by a model for higher-order terms including discretization and finite-volume effects (61 parameters for 39 data points supplemented by Bayesian priors). Their final result is $f_{K^\pm}/f_{\pi^\pm} = 1.1916(15)_{\text{stat}}(12)_{\text{a}^2}(1)_{FV}(10)$, where the errors are statistical, due to the continuum extrapolation, due to finite-volume effects and the last error contains the combined uncertainties from the chiral extrapolation, the scale-setting uncertainty, the experimental input in terms of f_{π^+} and from the uncertainty in m_u/m_d.

In the previous edition of the FLAG review [1] the error budget of HPQCD 13A was compared with the one of MILC 13A and discussed in details. It was pointed out that,

despite the large overlap in primary lattice data, both collaborations arrive at surprisingly different error budgets. The same still holds when the comparison is made between HPQCD 13A and FNAL/MILC 14A.

Concerning the cutoff dependence, the finest lattice included into MILC's analysis is $a = 0.06$ fm while the finest lattice in HPQCD's case is $a = 0.09$ fm and both collaborations allow for taste-breaking terms in their analyses. MILC estimates the residual systematic after extrapolating to the continuum limit by taking the split between the result of an extrapolation with up to quartic and only up to quadratic terms in a as their systematic. HPQCD on the other hand models cutoff effects within their global fit ansatz up to including terms in a^8, using priors for the unknown coefficients and without including the spread in the central values obtained from different ansätze into the systematic errors. In this way HPQCD arrives at a systematic error due to the continuum limit which is smaller than MILC's estimate by about a factor $\simeq 1.8$.

Turning to finite-volume effects, NLO staggered chiral perturbation theory (MILC) or continuum chiral perturbation theory (HPQCD) was used for correcting the lattice data towards the infinite-volume limit. MILC then compared the finite-volume correction to the one obtained by the NNLO expression and took the difference as their estimate for the residual finite-volume error. In addition they checked the compatibility of the effective-theory predictions (NLO continuum, staggered and NNLO continuum chiral perturbation theory) against lattice data of different spacial extent. The final verdict is that the related residual systematic uncertainty on $f_{K^\pm}/f_{\pi^\pm}$ made by MILC is larger by an order of magnitude than the one made by HPQCD.

Adding in quadrature all the uncertainties one gets: $f_{K^\pm}/f_{\pi^\pm} = 1.1916(22)$ (HPQCD 13A) and $f_{K^\pm}/f_{\pi^\pm} = 1.1960(24)$[4] (FNAL/MILC 14A). It can be seen that the total errors turn out to be very similar, but the central values seem to show a slight tension of about two standard deviations. While FLAG is looking forward to independent confirmations of the result for $f_{K^\pm}/f_{\pi^\pm}$ at the same level of precision, we evaluate the FLAG average using a two-step procedure. bf First, the HPQCD 13A and FNAL/MILC 14A are averaged assuming a 100% statistical and systematic correlations, obtaining $f_{K^\pm}/f_{\pi^\pm} = 1.1936(31)$, where, following the prescription of Sec. 2.3, the error has been inflated by the factor $\sqrt{(\chi^2/\mathrm{dof})} \simeq \sqrt{1.8}$ as a result of the tension between the two central values. Then, the above finding is averaged with the (uncorrelated) ETM 14E result, obtaining

$$\text{direct, } N_f = 2+1+1: \qquad f_{K^\pm}/f_{\pi^\pm} = 1.193(3) \qquad \text{Refs. [67, 68, 70]}. \tag{61}$$

For $N_f = 2+1$ one new result, RBC/UKQCD 14B, is now eligible to enter the FLAG average and it superseeds RBC/UKQCD 12 thanks to new simulations at finer lattice spacings and more lattice volumes with pion masses down to 140 MeV. Here we limit ourselves to note that for $N_f = 2+1$ MILC 10 and HPQCD/UKQCD 07 are based on staggered fermions, BMW 10 has used improved Wilson fermions and RBC/UKQCD 14B's result is based on the domain-wall formulation. In contrast to FNAL/MILC 14A and RBC/UKQCD 14B the other simulations are for unphysical values of the light-quark masses (corresponding to smallest pion masses in the range $240 - 260$ MeV in the case of MILC 10 and HPQCD/UKQCD 07) and therefore slightly more sophisticated extrapolations needed to be controlled. Various ansätze for the mass and cutoff dependence comprising $SU(2)$ and $SU(3)$ chiral perturbation

[4] Here we have symmetrized the asymmetric systematic error and shifted the central value by half the difference as will be done throughout this section.

theory or simply polynomials were used and compared in order to estimate the model dependence. While BMW 10 and RBC/UKQCD 14B are entirely independent computations, subsets of the MILC gauge ensembles used by MILC 10 and HPQCD/UKQCD 07 are the same. MILC 10 is certainly based on a larger and more advanced set of gauge configurations than HPQCD/UKQCD 07. This allows them for a more reliable estimation of systematic effects. In this situation we consider both statistical and systematic uncertainties to be correlated.

For $N_f = 2$ no new result enters the corresponding FLAG average with respect to the previous edition of the FLAG review [1], which therefore remains the ETM 09 result, which has simulated twisted-mass fermions down to (charged) pion masses equal to 260 MeV.

Before determining the average for $f_{K^\pm}/f_{\pi^\pm}$, which should be used for applications to Standard-Model phenomenology, we apply the isospin correction individually to all those results which have been published in the isospin-symmetric limit, i.e. BMW 10, HPQCD/UKQCD 07 and RBC/UKQCD 14B at $N_f = 2+1$ and ETM 09 at $N_f = 2$. To this end, as in the previous edition of the FLAG review [1], we make use of NLO $SU(3)$ chiral perturbation theory [52, 103], which predicts

$$\frac{f_{K^\pm}}{f_{\pi^\pm}} = \frac{f_K}{f_\pi}\,\sqrt{1+\delta_{SU(2)}}\,, \tag{62}$$

where [103]

$$\delta_{SU(2)} \;\approx\; \sqrt{3}\,\epsilon_{SU(2)}\left[-\tfrac{4}{3}\,(f_K/f_\pi - 1) + \tfrac{2}{3(4\pi)^2 f_0^2}\left(M_K^2 - M_\pi^2 - M_\pi^2 \ln\tfrac{M_K^2}{M_\pi^2}\right)\right]. \tag{63}$$

We use as input $\epsilon_{SU(2)} = \sqrt{3}/4/R$ with the FLAG result for R of Eq. (36), $F_0 = f_0/\sqrt{2} = 80(20)$ MeV, $M_\pi = 135$ MeV and $M_K = 495$ MeV (we decided to choose a conservative uncertainty on f_0 in order to reflect the magnitude of potential higher-order corrections). The results are reported in Tab. 15, where in the last column the last error is due to the isospin correction (the remaining errors are quoted in the same order as in the original data).

	f_K/f_π	$\delta_{SU(2)}$	$f_{K^\pm}/f_{\pi^\pm}$
HPQCD/UKQCD 07	1.189(2)(7)	-0.0040(7)	1.187(2)(7)(2)
BMW 10	1.192(7)(6)	-0.0041(7)	1.190(7)(6)(2)
RBC/UKQCD 14B	1.1945(45)	-0.0043(9)	1.1919(45)(26)

Table 15: Values of the $SU(2)$ isospin-breaking correction $\delta_{SU(2)}$ applied to the lattice data for f_K/f_π , entering the FLAG average at $N_f = 2+1$, for obtaining the corrected charged ratio $f_{K^\pm}/f_{\pi^\pm}$.

For $N_f = 2$ a dedicated study of the strong-isospin correction in lattice QCD does exist. The (updated) result of the RM123 collaboration [31] amounts to $\delta_{SU(2)} = -0.0080(4)$ and we use this result for the isospin correction of the ETM 09 result at $N_f = 2$.

Note that the RM123 value for the strong-isospin correction is almost incompatible with the results based on $SU(3)$ chiral perturbation theory, $\delta_{SU(2)} = -0.004(1)$ (see Tab. 15). Moreover, for $N_f = 2+1+1$ HPQCD 13A [70] and ETM 14E [67] estimate a value for $\delta_{SU(2)}$ equal to $-0.0054(14)$ and $-0.0080(38)$, respectively. One would not expect the strange and

heavier sea-quark contributions to be responsible for such a large effect. Whether higher-order effects in chiral perturbation theory or other sources are responsible still needs to be understood. More lattice QCD simulations of $SU(2)$ isospin-breaking effects are therefore required. To remain on the conservative side we add a 100% error to the correction based on $SU(3)$ chiral perturbation theory. For further analyses we add (in quadrature) such an uncertainty to the systematic error.

Using the results of Tab. 15 for $N_f = 2+1$ we obtain

$$\text{direct, } N_f = 2+1+1: \quad f_{K^\pm}/f_{\pi^\pm} = 1.193(3) \quad \text{Refs. [67, 68, 70]}, \tag{64}$$

$$\text{direct, } N_f = 2+1: \quad f_{K^\pm}/f_{\pi^\pm} = 1.192(4) \quad \text{Refs. [76, 79, 83, 90]}, \tag{65}$$

$$\text{direct, } N_f = 2: \quad f_{K^\pm}/f_{\pi^\pm} = 1.205(6)(17) \quad \text{Ref. [95]}, \tag{66}$$

for QCD with broken isospin.

It is instructive to convert the above results for $f_+(0)$ and $f_{K^\pm}/f_{\pi^\pm}$ into a corresponding range for the CKM matrix elements $|V_{ud}|$ and $|V_{us}|$, using the relations (54). Consider first the results for $N_f = 2+1+1$. The range for $f_+(0)$ in Eq. (58) is mapped into the interval $|V_{us}| = 0.2231(7)$, depicted as a horizontal red band in Fig. 8, while the one for $f_{K^\pm}/f_{\pi^\pm}$ in Eq. (64) is converted into $|V_{us}|/|V_{ud}| = 0.2313(7)$, shown as a tilted red band. The red ellipse is the intersection of these two bands and represents the 68% likelihood contour,[5] obtained by treating the above two results as independent measurements. Repeating the exercise for $N_f = 2+1$ and $N_f = 2$ leads to the green and blue ellipses, respectively. The plot indicates a slight tension of both the $N_f = 2+1+1$ and $N_f = 2+1$ results with the one from nuclear β decay.

4.4 Tests of the Standard Model

In the Standard Model, the CKM matrix is unitary. In particular, the elements of the first row obey

$$|V_u|^2 \equiv |V_{ud}|^2 + |V_{us}|^2 + |V_{ub}|^2 = 1\,. \tag{67}$$

The tiny contribution from $|V_{ub}|$ is known much better than needed in the present context: $|V_{ub}| = 4.13(49)\cdot 10^{-3}$ [5]. In the following, we first discuss the evidence for the validity of the relation (67) and only then use it to analyse the lattice data within the Standard Model.

In Fig. 8, the correlation between $|V_{ud}|$ and $|V_{us}|$ imposed by the unitarity of the CKM matrix is indicated by a dotted line (more precisely, in view of the uncertainty in $|V_{ub}|$, the correlation corresponds to a band of finite width, but the effect is too small to be seen here). The plot shows that there is a slight tension with unitarity in the data for $N_f = 2+1+1$: Numerically, the outcome for the sum of the squares of the first row of the CKM matrix reads $|V_u|^2 = 0.9798(82)$, which deviates from unity at the level of $\simeq 2.5$ standard deviations. Still, it is fair to say that at this level the Standard Model passes a nontrivial test that exclusively involves lattice data and well-established kaon decay branching ratios. Combining the lattice results for $f_+(0)$ and $f_{K^\pm}/f_{\pi^\pm}$ in Eqs. (58) and (64) with the β decay value of $|V_{ud}|$ quoted in Eq. (55), the test sharpens considerably: the lattice result for $f_+(0)$ leads to $|V_u|^2 = 0.9988(5)$, which highlights again a $\simeq 2.4\sigma$-tension with unitarity, while the one for $f_{K^\pm}/f_{\pi^\pm}$ implies $|V_u|^2 = 0.9998(5)$, confirming the first-row CKM unitarity below the permille level.

[5] Note that the ellipses shown in Fig. 5 of both Ref. [104] and Ref. [1] correspond instead to the 39% likelihood contours. Note also that in Ref. [1] the likelihood was erroneously stated to be 68% rather than 39%.

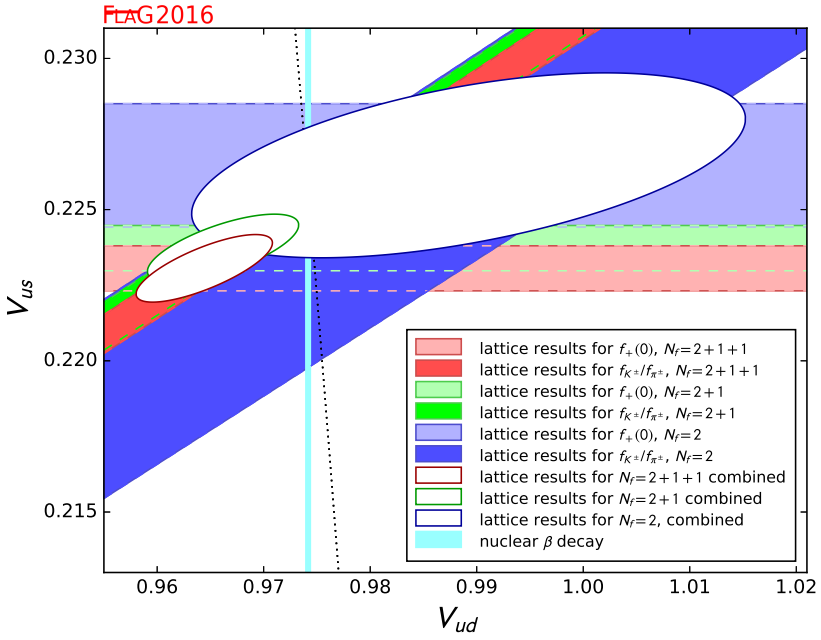

Figure 8: The plot compares the information for $|V_{ud}|$, $|V_{us}|$ obtained on the lattice with the experimental result extracted from nuclear β transitions. The dotted line indicates the correlation between $|V_{ud}|$ and $|V_{us}|$ that follows if the CKM-matrix is unitary.

The situation is similar for $N_f = 2 + 1$: with the lattice data alone one has $|V_u|^2 = 0.9835(92)$, which deviates from unity at the level of $\simeq 1.8$ standard deviations. Combining the lattice results for $f_+(0)$ and $f_{K^\pm}/f_{\pi^\pm}$ in Eqs. (59) and (65) with the β decay value of $|V_{ud}|$, the test sharpens again considerably: the lattice result for $f_+(0)$ leads to $|V_u|^2 = 0.9991(5)$, implying again a $\simeq 1.8\sigma$-tension with unitarity, while the one for $f_{K^\pm}/f_{\pi^\pm}$ implies $|V_u|^2 = 0.9999(5)$, thus confirming again CKM unitarity below the permille level.

Repeating the analysis for $N_f = 2$, we find $|V_u|^2 = 1.029(34)$ with the lattice data alone. This number is fully compatible with unity and perfectly consistent with the value of $|V_{ud}|$ found in nuclear β decay: combining this value with the result (60) for $f_+(0)$ yields $|V_u|^2 = 1.0003(10)$, combining it with the data (66) on $f_{K^\pm}/f_{\pi^\pm}$ gives $|V_u|^2 = 0.9988(15)$.

Note that the above tests also offer a check of the basic hypothesis that underlies our analysis: we are assuming that the weak interaction between the quarks and the leptons is governed by the same Fermi constant as the one that determines the strength of the weak interaction among the leptons and the lifetime of the muon. In certain modifications of the Standard Model, this is not the case. In those models it need not be true that the rates of the decays $\pi \to \ell\nu$, $K \to \ell\nu$ and $K \to \pi\ell\nu$ can be used to determine the matrix elements $|V_{ud} f_\pi|$, $|V_{us} f_K|$ and $|V_{us} f_+(0)|$, respectively and that $|V_{ud}|$ can be measured in nuclear β decay. The fact that the lattice data are consistent with unitarity and with the value of $|V_{ud}|$ found in nuclear β decay indirectly also checks the equality of the Fermi constants.

4.5 Analysis within the Standard Model

The Standard Model implies that the CKM matrix is unitary. The precise experimental constraints quoted in (54) and the unitarity condition (67) then reduce the four quantities $|V_{ud}|, |V_{us}|, f_+(0), f_{K^\pm}/f_{\pi^\pm}$ to a single unknown: any one of these determines the other three within narrow uncertainties.

Fig. 9 shows that the results obtained for $|V_{us}|$ and $|V_{ud}|$ from the data on $f_{K^\pm}/f_{\pi^\pm}$ (squares) are quite consistent with the determinations via $f_+(0)$ (triangles). In order to calculate the corresponding average values, we restrict ourselves to those determinations that we have considered best in Sec. 4.3. The corresponding results for $|V_{us}|$ are listed in Tab. 16 (the error in the experimental numbers used to convert the values of $f_+(0)$ and $f_{K^\pm}/f_{\pi^\pm}$ into values for $|V_{us}|$ is included in the statistical error).

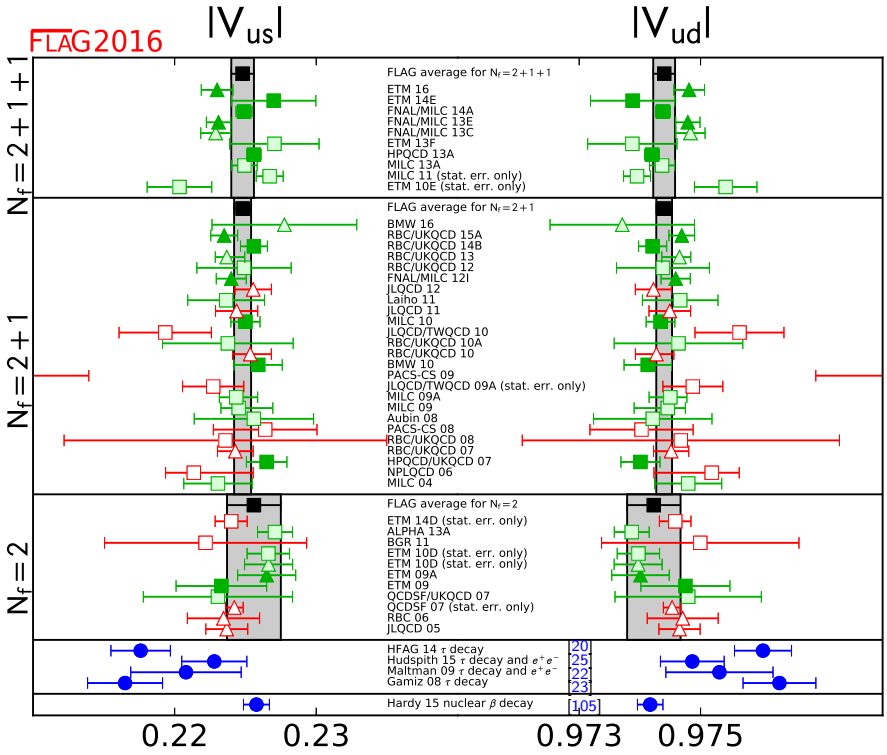

Figure 9: Results for $|V_{us}|$ and $|V_{ud}|$ that follow from the lattice data for $f_+(0)$ (triangles) and $f_{K^\pm}/f_{\pi^\pm}$ (squares), on the basis of the assumption that the CKM matrix is unitary. The black squares and the grey bands represent our estimates, obtained by combining these two different ways of measuring $|V_{us}|$ and $|V_{ud}|$ on a lattice. For comparison, the figure also indicates the results obtained if the data on nuclear β decay and τ decay are analysed within the Standard Model.

For $N_f = 2+1+1$ we consider the data both for $f_+(0)$ and $f_{K^\pm}/f_{\pi^\pm}$, treating ETM 16 and ETM 14E on the one hand and FNAL/MILC 13E, FNAL/MILC 14A and HPQCD 13A on the other hand, as statistically correlated according to the prescription of Sec. 2.3. We obtain $|V_{us}| = 0.2248(8)$, where the error includes the inflation factor due the value of $\chi^2/\text{dof} \simeq 2.4$.

Collaboration	Ref.	N_f	from	$\lvert V_{us}\rvert$	$\lvert V_{ud}\rvert$
ETM 16	[34]	$2+1+1$	$f_+(0)$	0.2230(11)(2)	0.97481(25)(5)
FNAL/MILC 13E	[35]	$2+1+1$	$f_+(0)$	0.2231(7)(5)	0.97479(16)(12)
ETM 14E	[67]	$2+1+1$	$f_{K^\pm}/f_{\pi^\pm}$	0.2270(22)(20)	0.97388(51)(47)
FNAL/MILC 14A	[68]	$2+1+1$	$f_{K^\pm}/f_{\pi^\pm}$	0.2249(4)(4)	0.97438(8)(9)
HPQCD 13A	[70]	$2+1+1$	$f_{K^\pm}/f_{\pi^\pm}$	0.2256(4)(3)	0.97420(10)(7)
RBC/UKQCD 15A	[38]	$2+1$	$f_+(0)$	0.2235(9)(3)	0.97469(20)(7)
FNAL/MILC 12I	[40]	$2+1$	$f_+(0)$	0.2240(7)(8)	0.97459(16)(18)
RBC/UKQCD 14B	[76]	$2+1$	$f_{K^\pm}/f_{\pi^\pm}$	0.2256(3)(9)	0.97421(7)(22)
MILC 10	[79]	$2+1$	$f_{K^\pm}/f_{\pi^\pm}$	0.2250(5)(9)	0.97434(11)(21)
BMW 10	[83]	$2+1$	$f_{K^\pm}/f_{\pi^\pm}$	0.2259(13)(11)	0.97413(30)(25)
HPQCD/UKQCD 07	[90]	$2+1$	$f_{K^\pm}/f_{\pi^\pm}$	0.2265(6)(13)	0.97401(14)(29)
ETM 09A	[46]	2	$f_+(0)$	0.2265(14)(15)	0.97401(33)(34)
ETM 09	[95]	2	$f_{K^\pm}/f_{\pi^\pm}$	0.2233(11)(30)	0.97475(25)(69)

Table 16: Values of $|V_{us}|$ and $|V_{ud}|$ obtained from the lattice determinations of either $f_+(0)$ or $f_{K^\pm}/f_{\pi^\pm}$ assuming CKM unitarity. The first (second) number in brackets represents the statistical (systematic) error.

This result is indicated on the left hand side of Fig. 9 by the narrow vertical band. In the case $N_f = 2+1$ we consider MILC 10, FNAL/MILC 12I and HPQCD/UKQCD 07 on the one hand and RBC/UKQCD 14B and RBC/UKQCD 15A on the other hand, as mutually statistically correlated, since the analysis in the two cases starts from partly the same set of gauge ensembles. In this way we arrive at $|V_{us}| = 0.2248(6)$ with $\chi^2/\text{dof} \simeq 1.0$. For $N_f = 2$ we consider ETM 09A and ETM 09 as statistically correlated, obtaining $|V_{us}| = 0.2256(19)$ with $\chi^2/\text{dof} \simeq 0.7$. The figure shows that the result obtained for the data with $N_f = 2$, $N_f = 2+1$ and $N_f = 2+1+1$ are consistent with each other.

Alternatively, we can solve the relations for $|V_{ud}|$ instead of $|V_{us}|$. Again, the result $|V_{ud}| = 0.97440(18)$ which follows from the lattice data with $N_f = 2+1+1$ is perfectly consistent with the values $|V_{ud}| = 0.97440(13)$ and $|V_{ud}| = 0.97423(44)$ obtained from the data with $N_f = 2+1$ and $N_f = 2$, respectively. The reduction of the uncertainties in the result for $|V_{ud}|$ due to CKM unitarity is to be expected from Fig. 8: the unitarity condition reduces the region allowed by the lattice results to a nearly vertical interval.

Next, we determine the values of $f_+(0)$ and $f_{K^\pm}/f_{\pi^\pm}$ that follow from our determinations of $|V_{us}|$ and $|V_{ud}|$ obtained from the lattice data within the Standard Model. We find $f_+(0) = 0.9631(39)$ for $N_f = 2+1+1$, $f_+(0) = 0.9631(31)$ for $N_f = 2+1$, $f_+(0) = 0.9597(83)$ for $N_f = 2$ and $f_{K^\pm}/f_{\pi^\pm} = 1.196(4)$ for $N_f = 2+1+1$, $f_{K^\pm}/f_{\pi^\pm} = 1.196(3)$ for $N_f = 2+1$, $f_{K^\pm}/f_{\pi^\pm} = 1.192(9)$ for $N_f = 2$, respectively. These results are collected in the upper half of Tab. 17. In the lower half of the table, we list the analogous results found by working out the consequences of the CKM unitarity using the values of $|V_{ud}|$ and $|V_{us}|$ obtained from nuclear β decay and τ decay, respectively. The comparison shows that the lattice result for

$|V_{ud}|$ not only agrees very well with the totally independent determination based on nuclear β transitions, but is also remarkably precise. On the other hand, the values of $|V_{ud}|$, $f_+(0)$ and $f_{K^\pm}/f_{\pi^\pm}$ which follow from the τ-decay data if the Standard Model is assumed to be valid, are not all in agreement with the lattice results for these quantities. The disagreement is reduced considerably if the analysis of the τ data is supplemented with experimental results on electroproduction [22]: the discrepancy then amounts to little more than one standard deviation. The disagreement seems to disappear when recent implementations of the relevant sum rules are considered [25].

	Ref.	$\lvert V_{us}\rvert$	$\lvert V_{ud}\rvert$	$f_+(0)$	$f_{K^\pm}/f_{\pi^\pm}$
$N_f = 2+1+1$		0.2248(8)	0.97440(18)	0.9631(39)	1.196(4)
$N_f = 2+1$		0.2248(6)	0.97440(13)	0.9631(31)	1.196(3)
$N_f = 2$		0.2256(19)	0.97423(44)	0.9597(83)	1.192(9)
β decay	[9]	0.2258(9)	0.97417(21)	0.9588(42)	1.191(4)
τ decay	[23]	0.2165(26)	0.9763(6)	1.0000(122)	1.245(12)
τ decay + e^+e^-	[22]	0.2208(39)	0.9753(9)	0.9805(174)	1.219(18)
τ decay + e^+e^-	[25]	0.2238(23)	0.9749(5)	0.9674(101)	1.202(10)

Table 17: The upper half of the table shows our final results for $|V_{us}|$, $|V_{ud}|$, $f_+(0)$ and $f_{K^\pm}/f_{\pi^\pm}$, which are obtained by analysing the lattice data within the Standard Model. For comparison, the lower half lists the values that follow if the lattice results are replaced by the experimental results on nuclear β decay and τ decay, respectively.

4.6 Direct determination of $f_{K^\pm}$ and $f_{\pi^\pm}$

It is useful for flavour physics studies to provide not only the lattice average of $f_{K^\pm}/f_{\pi^\pm}$, but also the average of the decay constant $f_{K^\pm}$. The case of the decay constant $f_{\pi^\pm}$ is different, since the experimental value of this quantity is often used for setting the scale in lattice QCD (see Appendix A.2). However, the physical scale can be set in different ways, namely by using as input the mass of the Ω-baryon (m_Ω) or the Υ-meson spectrum (ΔM_Υ), which are less sensitive to the uncertainties of the chiral extrapolation in the light-quark mass with respect to $f_{\pi^\pm}$. In such cases the value of the decay constant $f_{\pi^\pm}$ becomes a direct prediction of the lattice-QCD simulations. It is therefore interesting to provide also the average of the decay constant $f_{\pi^\pm}$, obtained when the physical scale is set through another hadron observable, in order to check the consistency of different scale setting procedures.

Our compilation of the values of $f_{\pi^\pm}$ and $f_{K^\pm}$ with the corresponding colour code is presented in Tab. 18. With respect to the case of $f_{K^\pm}/f_{\pi^\pm}$ we have added two columns indicating which quantity is used to set the physical scale and the possible use of a renormalization constant for the axial current. Indeed, for several lattice formulations the use of the nonsinglet axial-vector Ward identity allows to avoid the use of any renormalization constant.

One can see that the determinations of $f_{\pi^\pm}$ and $f_{K^\pm}$ suffer from larger uncertainties with respect to the ones of the ratio $f_{K^\pm}/f_{\pi^\pm}$, which is less sensitive to various systematic

effects (including the uncertainty of a possible renormalization constant) and, moreover, is not exposed to the uncertainties of the procedure used to set the physical scale.

According to the FLAG rules, for $N_f = 2+1+1$ three data sets can form the average of $f_{K^\pm}$ only: ETM 14E [67], FNAL/MILC 14A [68] and HPQCD 13A [70]. Following the same procedure already adopted in Sec. 4.3 in the case of the ratio of the decay constant we treat FNAL/MILC 14A and HPQCD 13A as statistically correlated. For $N_f = 2+1$ three data sets can form the average of $f_{\pi^\pm}$ and $f_{K^\pm}$: RBC/UKQCD 14B [76] (update of RBC/UKQCD 12), HPQCD/UKQCD 07 [90] and MILC 10 [79], which is the latest update of the MILC program. We consider HPQCD/UKQCD 07 and MILC 10 as statistically correlated and use the prescription of Sec. 2.3 to form an average. For $N_f = 2$ the average cannot be formed for $f_{\pi^\pm}$, and only one data set (ETM 09) satisfies the FLAG rules in the case of $f_{K^\pm}$.

Thus, our estimates read

$$N_f = 2+1: \qquad f_{\pi^\pm} = 130.2\ (0.8)\ \text{MeV} \qquad \text{Refs. [76, 79, 90]}, \tag{68}$$

$$\begin{aligned} N_f &= 2+1+1: \quad f_{K^\pm} = 155.7\ (0.3)\ \text{MeV} \quad \text{Refs. [67, 68, 70]}, \\ N_f &= 2+1: \quad f_{K^\pm} = 155.7\ (0.7)\ \text{MeV} \quad \text{Refs. [76, 79, 90]}, \\ N_f &= 2: \quad f_{K^\pm} = 157.5\ (2.4)\ \text{MeV} \quad \text{Ref. [95]}. \end{aligned} \tag{69}$$

The lattice results of Tab. 18 and our estimates (68-69) are reported in Fig. 10. The latter ones agree within the errors with the latest experimental determinations of f_π and f_K from the PDG [5]:

$$f_{\pi^\pm}^{(PDG)} = 130.41\ (0.20)\ \text{MeV} \qquad , \qquad f_{K^\pm}^{(PDG)} = 156.2\ (0.7)\ \text{MeV}\ . \tag{70}$$

Moreover the values of $f_{\pi^\pm}$ and $f_{K^\pm}$ quoted by the PDG are obtained assuming Eq. (55) for the value of $|V_{ud}|$ and adopting the average of FNAL/MILC 12I and RBC-UKQCD 10 results for $f_+(0)$.

Collaboration	Ref.	N_f	publication status	chiral extrapolation	continuum extrapolation	finite-volume errors	renormalization	physical scale	$SU(2)$ breaking	$f_{\pi^\pm}$	$f_{K^\pm}$
ETM 14E	[67]	2+1+1	A	○	★	○	na	f_π		–	154.4(1.5)(1.3)
FNAL/MILC 14A	[68]	2+1+1	A	★	★	★	na	f_π		–	$155.92(13)(^{+34}_{-23})$
HPQCD 13A	[70]	2+1+1	A	★	○	★	na	f_π		–	155.37(20)(27)
MILC 13A	[71]	2+1+1	A	★	○	★	na	f_π		–	155.80(34)(54)
ETM 10E	[73]	2+1+1	C	○	○	○	na	f_π	✓	–	159.6(2.0)
JLQCD 15C	[106]	2+1	C	○	★	★	NPR	t_0		$125.7(7.4)_{\rm stat}$	
RBC/UKQCD 14B	[76]	2+1	A	★	★	★	NPR	m_Ω	✓	130.19(89)	155.18(89)
RBC/UKQCD 12	[77]	2+1	A	★	○	★	NPR	m_Ω	✓	127.1(2.7)(2.7)	152.1(3.0)(1.7)
Laiho 11	[78]	2+1	C	○	★	○	na	†		130.53(87)(210)	156.8(1.0)(1.7)
MILC 10	[79]	2+1	C	○	★	★	na	†		129.2(4)(14)	–
MILC 10	[79]	2+1	C	○	★	★	na	f_π		–	$156.1(4)(^{+6}_{-9})$
JLQCD/TWQCD 10	[80]	2+1	C	○	■	★	na	m_Ω	✓	$118.5(3.6)_{\rm stat}$	$145.7(2.7)_{\rm stat}$
RBC/UKQCD 10A	[81]	2+1	A	○	○	★	NPR	m_Ω	✓	124(2)(5)	148.8(2.0)(3.0)
PACS-CS 09	[82]	2+1	A	★	■	■	NPR	m_Ω	✓	124.1(8.5)(0.8)	165.0(3.4)(1.1)
JLQCD/TWQCD 09A	[84]	2+1	C	○	■	■	na	f_π	✓	–	$156.9(5.5)_{\rm stat}$
MILC 09A	[85]	2+1	C	○	★	★	na	ΔM_Υ		128.0(0.3)(2.9)	153.8(0.3)(3.9)
MILC 09A	[85]	2+1	C	○	★	★	na	f_π		–	156.2(0.3)(1.1)
MILC 09	[86]	2+1	A	○	★	★	na	ΔM_Υ		$128.3(0.5)(^{+2.4}_{-3.5})$	$154.3(0.4)(^{+2.1}_{-3.4})$
MILC 09	[86]	2+1	A	○	★	★	na	f_π			$156.5(0.4)(^{+1.0}_{-2.7})$
Aubin 08	[87]	2+1	C	○	○	○	na	ΔM_Υ		129.1(1.9)(4.0)	153.9(1.7)(4.4)
PACS-CS 08, 08A	[27, 88]	2+1	A	★	■	■	1lp	m_Ω	✓	$134.0(4.2)_{\rm stat}$	$159.0(3.1)_{\rm stat}$
RBC/UKQCD 08	[89]	2+1	A	○	■	★	NPR	m_Ω	✓	124.1(3.6)(6.9)	149.4(3.6)(6.3)
HPQCD/UKQCD 07	[90]	2+1	A	○	○	○	na	ΔM_Υ	✓	132(2)	156.7(0.7)(1.9)
MILC 04	[66]	2+1	A	○	○	○	na	ΔM_Υ		129.5(0.9)(3.5)	156.6(1.0)(3.6)
ETM 14D	[92]	2	C	★	■	○	na	f_π	✓	–	$153.3(7.5)_{\rm stat}$
TWQCD 11	[107]	2	P	★	■	■	na	$r_0{}^*$		$127.3(1.7)(2.0)^{**}$	–
ETM 09	[95]	2	A	○	★	○	na	f_π	✓	–	$157.5(0.8)(2.0)(1.1)^{\dagger\dagger}$
JLQCD/TWQCD 08A	[108]	2	A	○	■	■	na	r_0		$119.6(3.0)(^{+6.5}_{-1.0})^{**}$	–

The label 'na' indicates the lattice calculations which do not require the use of any renormalization constant for the axial current, while the label 'NPR' ('1lp') signals the use of a renormalization constant calculated nonperturbatively (at 1-loop order in perturbation theory).

† The ratios of lattice spacings within the ensembles were determined using the quantity r_1. The conversion to physical units was made on the basis of Ref. [109] and we note that such a determination depends on the experimental value of the pion decay constant

†† Errors are (stat+chiral)($a \neq 0$)(finite size).

* The ratio f_π/M_π was used as experimental input to fix the light-quark mass.

** $L_{\rm min} < 2$fm in these simulations.

Table 18: Colour code for the lattice data on $f_{\pi^\pm}$ and $f_{K^\pm}$ together with information on the way the lattice spacing was converted to physical units and on whether or not an isospin-breaking correction has been applied to the quoted result (see Sec. 4.3). The numerical values are listed in MeV units.

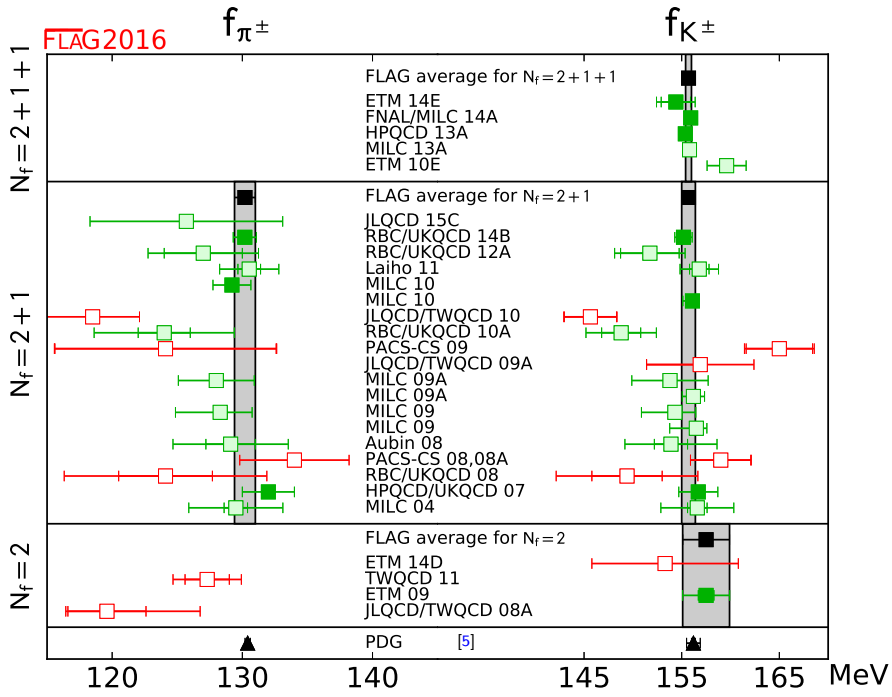

Figure 10: Values of f_π and f_K. The black squares and grey bands indicate our estimates (68) and (69). The black triangles represent the experimental values quoted by the PDG, see Eq. (70).

References

[1] [FLAG 13] S. Aoki, Y. Aoki, C. Bernard, T. Blum, G. Colangelo et al., *Review of lattice results concerning low-energy particle physics*, *Eur.Phys.J.* **C74** (2014) 2890, [1310.8555].

[2] M. Moulson, *Experimental determination of V_{us} from kaon decays*, in *8th International Workshop on the CKM Unitarity Triangle (CKM2014) Vienna, Austria, September 8-12, 2014*, 2014. 1411.5252.

[3] J. L. Rosner, S. Stone and R. S. Van de Water, *Leptonic Decays of Charged Pseudoscalar Mesons, in Review of Particle Physics [5] 2015 update*, 1509.02220.

[4] J. Gasser and G. R. S. Zarnauskas, *On the pion decay constant*, *Phys. Lett.* **B693** (2010) 122–128, [1008.3479].

[5] Particle Data Group collaboration, K. A. Olive et al., *Review of Particle Physics*, *Chin. Phys.* **C38** (2014) 090001 and 2015 update.

[6] J. Gasser, A. Rusetsky and I. Scimemi, *Electromagnetic corrections in hadronic processes*, *Eur. Phys. J.* **C32** (2003) 97–114, [hep-ph/0305260].

[7] A. Rusetsky, *Isospin symmetry breaking*, *PoS* **CD09** (2009) 071, [0910.5151].

[8] J. Gasser, *Theoretical progress on cusp effect and $K_{\ell 4}$ decays*, *PoS* **KAON07** (2008) 033, [0710.3048].

[9] J. C. Hardy and I. S. Towner, *Superallowed $0^+ \to 0^+$ nuclear decays: 2014 critical survey, with precise results for V_{ud} and CKM unitarity*, *Phys. Rev.* **C91** (2015) 025501, [1411.5987].

[10] I. S. Towner and J. C. Hardy, *An improved calculation of the isospin-symmetry-breaking corrections to superallowed Fermi β decay*, *Phys. Rev.* **C77** (2008) 025501, [0710.3181].

[11] G. A. Miller and A. Schwenk, *Isospin-symmetry-breaking corrections to superallowed Fermi β decay: formalism and schematic models*, *Phys. Rev.* **C78** (2008) 035501, [0805.0603].

[12] N. Auerbach, *Coulomb corrections to superallowed β decay in nuclei*, *Phys. Rev.* **C79** (2009) 035502, [0811.4742].

[13] H. Liang, N. Van Giai and J. Meng, *Isospin corrections for superallowed Fermi β decay in self-consistent relativistic random-phase approximation approaches*, *Phys. Rev.* **C79** (2009) 064316, [0904.3673].

[14] G. A. Miller and A. Schwenk, *Isospin-symmetry-breaking corrections to superallowed Fermi β decay: radial excitations*, *Phys. Rev.* **C80** (2009) 064319, [0910.2790].

[15] I. Towner and J. Hardy, *Comparative tests of isospin-symmetry-breaking corrections to superallowed $0^+ \to 0^+$ nuclear β decay*, *Phys.Rev.* **C82** (2010) 065501, [1007.5343].

[16] E. Gamiz, M. Jamin, A. Pich, J. Prades and F. Schwab, *Determination of m_s and $|V_{us}|$ from hadronic τ decays*, *JHEP* **01** (2003) 060, [hep-ph/0212230].

[17] E. Gamiz, M. Jamin, A. Pich, J. Prades and F. Schwab, *V_{us} and m_s from hadronic τ decays*, *Phys. Rev. Lett.* **94** (2005) 011803, [hep-ph/0408044].

[18] K. Maltman, *A mixed τ-electroproduction sum rule for V_{us}*, *Phys. Lett.* **B672** (2009) 257–263, [0811.1590].

[19] A. Pich and R. Kass, *talks given at CKM 2008*, http://ckm2008.roma1.infn.it.

[20] [HFAG 14] Y. Amhis et al., *Averages of b-hadron, c-hadron, and τ-lepton properties as of summer 2014*, 1412.7515.

[21] K. Maltman, C. E. Wolfe, S. Banerjee, J. M. Roney and I. Nugent, *Status of the hadronic τ determination of V_{us}*, *Int. J. Mod. Phys.* **A23** (2008) 3191–3195, [0807.3195].

[22] K. Maltman, C. E. Wolfe, S. Banerjee, I. M. Nugent and J. M. Roney, *Status of the hadronic τ decay determination of $|V_{us}|$*, *Nucl. Phys. Proc. Suppl.* **189** (2009) 175–180, [0906.1386].

[23] E. Gamiz, M. Jamin, A. Pich, J. Prades and F. Schwab, *Theoretical progress on the V_{us} determination from τ decays*, *PoS* **KAON07** (2008) 008, [0709.0282].

[24] E. Gamiz, *$|V_{us}|$ from hadronic τ decays, CKM 2012*, 1301.2206.

[25] R. J. Hudspith, R. Lewis, K. Maltman, C. E. Wolfe and J. Zanotti, *A resolution of the puzzle of low V_{us} values from inclusive flavor-breaking sum rule analyses of hadronic tau decay*, in *10th International Workshop on e+e- collisions from Phi to Psi (PHIPSI15) Hefei, Anhui, China, September 23-26, 2015*, 2015. 1511.08514.

[26] M. Antonelli et al., *An evaluation of $|V_{us}|$ and precise tests of the Standard Model from world data on leptonic and semileptonic kaon decays*, *Eur. Phys. J.* **C69** (2010) 399–424, [1005.2323].

[27] [PACS-CS 08] S. Aoki et al., *2+1 flavor lattice QCD toward the physical point*, *Phys. Rev.* **D79** (2009) 034503, [0807.1661].

[28] [RM123 11] G. M. de Divitiis, P. Dimopoulos, R. Frezzotti, V. Lubicz, G. Martinelli et al., *Isospin breaking effects due to the up-down mass difference in lattice QCD*, *JHEP* **1204** (2012) 124, [1110.6294].

[29] T. Ishikawa, T. Blum, M. Hayakawa, T. Izubuchi, C. Jung et al., *Full QED+QCD low-energy constants through reweighting*, *Phys.Rev.Lett.* **109** (2012) 072002, [1202.6018].

[30] T. Izubuchi, *Lattice QCD + QED - from Isospin breaking to g-2 light-by-light*, talk given at Lattice 2012, Cairns, Australia, http://www.physics.adelaide.edu.au/cssm/lattice2012.

[31] [RM123 13] G. M. de Divitiis, R. Frezzotti, V. Lubicz, G. Martinelli, R. Petronzio et al., *Leading isospin breaking effects on the lattice*, *Phys.Rev.* **D87** (2013) 114505, [1303.4896].

[32] N. Tantalo, *Isospin Breaking Effects on the Lattice*, *PoS* **LATTICE2013** (2014) 007, [1311.2797].

[33] A. Portelli, *Inclusion of isospin breaking effects in lattice simulations*, *PoS* **LATTICE2014** (2015) 013.

[34] [ETM 16] N. Carrasco, P. Lami, V. Lubicz, L. Riggio, S. Simula and C. Tarantino, *$K \to \pi$ semileptonic form factors with $N_f = 2 + 1 + 1$ twisted mass fermions*, *Phys. Rev.* **D93** (2016) 114512, [1602.04113].

[35] [FNAL/MILC 13E] A. Bazavov et al., *Determination of $|V_{us}|$ from a lattice-QCD calculation of the $K \to \pi \ell \nu$ semileptonic form factor with physical quark masses*, *Phys. Rev. Lett.* **112** (2014) 112001, [1312.1228].

[36] [FNAL/MILC 13C] E. Gamiz, A. Bazavov, C. Bernard, C. Bouchard, C. DeTar et al., *K semileptonic form factor with HISQ fermions at the physical point*, *PoS* **LATTICE2013** (2013) 395, [1311.7264].

[37] JLQCD 16] T. Kaneko, S. Aoki, G. Cossu, X. Feng, H. Fukaya, S. Hashimoto et al., *Chiral behavior of light meson form factors in 2+1 flavor QCD with exact chiral symmetry*, *PoS* **LATTICE2015** (2016) 325, [1601.07658].

[38] [RBC/UKQCD 15A] P.A. Boyle et al., *The kaon semileptonic form factor in N_f = 2 + 1 domain wall lattice QCD with physical light quark masses*, *JHEP* **1506** (2015) 164, [1504.01692].

[39] [RBC/UKQCD 13] P. A. Boyle, J. M. Flynn, N. Garron, A. Jüttner, C. T. Sachrajda et al., *The kaon semileptonic form factor with near physical domain wall quarks*, *JHEP* **1308** (2013) 132, [1305.7217].

[40] [FNAL/MILC 12I] A. Bazavov, C. Bernard, C. Bouchard, C. DeTar, D. Du et al., *Kaon semileptonic vector form factor and determination of $|V_{us}|$ using staggered fermions*, *Phys.Rev.* **D87** (2013) 073012, [1212.4993].

[41] [JLQCD 12] T. Kaneko et al., *Chiral behavior of kaon semileptonic form factors in lattice QCD with exact chiral symmetry*, *PoS* **LAT2012** (2012) 111, [1211.6180].

[42] [JLQCD 11] T. Kaneko et al., *Kaon semileptonic form factors in QCD with exact chiral symmetry*, *PoS* **LAT2011** (2011) 284, [1112.5259].

[43] [RBC/UKQCD 10] P. A. Boyle et al., *$K \to \pi$ form factors with reduced model dependence*, *Eur.Phys.J.* **C69** (2010) 159–167, [1004.0886].

[44] [RBC/UKQCD 07] P. A. Boyle, A. Jüttner, R. Kenway, C. Sachrajda, S. Sasaki et al., *K_{l3} semileptonic form-factor from 2+1 flavour lattice QCD*, *Phys.Rev.Lett.* **100** (2008) 141601, [0710.5136].

[45] [ETM 10D] V. Lubicz, F. Mescia, L. Orifici, S. Simula and C. Tarantino, *Improved analysis of the scalar and vector form factors of kaon semileptonic decays with $N_f = 2$ twisted-mass fermions*, *PoS* **LAT2010** (2010) 316, [1012.3573].

[46] [ETM 09A] V. Lubicz, F. Mescia, S. Simula and C. Tarantino, *$K \to \pi \ell \nu$ semileptonic form factors from two-flavor lattice QCD*, *Phys. Rev.* **D80** (2009) 111502, [0906.4728].

[47] [QCDSF 07] D. Brömmel et al., *Kaon semileptonic decay form factors from $N_f = 2$ non-perturbatively $O(a)$-improved Wilson fermions*, *PoS* **LAT2007** (2007) 364, [0710.2100].

[48] [RBC 06] C. Dawson, T. Izubuchi, T. Kaneko, S. Sasaki and A. Soni, *Vector form factor in K_{l3} semileptonic decay with two flavors of dynamical domain-wall quarks*, *Phys. Rev.* **D74** (2006) 114502, [hep-ph/0607162].

[49] [JLQCD 05] N. Tsutsui et al., *Kaon semileptonic decay form factors in two-flavor QCD*, *PoS* **LAT2005** (2006) 357, [hep-lat/0510068].

[50] M. Ademollo and R. Gatto, *Nonrenormalization theorem for the strangeness violating vector currents*, *Phys. Rev. Lett.* **13** (1964) 264–265.

[51] G. Furlan, F. Lannoy, C. Rossetti and G. Segré, *Symmetry-breaking corrections to weak vector currents*, *Nuovo Cim.* **38** (1965) 1747.

[52] J. Gasser and H. Leutwyler, *Chiral perturbation theory: expansions in the mass of the strange quark*, *Nucl. Phys.* **B250** (1985) 465.

[53] J. Gasser and H. Leutwyler, *Low-energy expansion of meson form factors*, *Nucl. Phys.* **B250** (1985) 517–538.

[54] C. Bernard, J. Bijnens and E. Gamiz, *Semileptonic kaon decay in staggered chiral perturbation theory*, *Phys. Rev.* **D89** (2014) 054510, [1311.7511].

[55] [RBC 08] J. M. Flynn and C. T. Sachrajda, *SU(2) chiral perturbation theory for $K_{\ell 3}$ decay amplitudes*, *Nucl. Phys.* **B812** (2009) 64–80, [0809.1229].

[56] A. Kastner and H. Neufeld, *The K_{l3} scalar form factors in the Standard Model*, *Eur. Phys. J.* **C57** (2008) 541–556, [0805.2222].

[57] V. Cirigliano et al., *The Green function and SU(3) breaking in K_{l3} decays*, *JHEP* **04** (2005) 006, [hep-ph/0503108].

[58] M. Jamin, J. A. Oller and A. Pich, *Order p^6 chiral couplings from the scalar $K\pi$ form factor*, *JHEP* **02** (2004) 047, [hep-ph/0401080].

[59] J. Bijnens and P. Talavera, *K_{l3} decays in chiral perturbation theory*, *Nucl. Phys.* **B669** (2003) 341–362, [hep-ph/0303103].

[60] H. Leutwyler and M. Roos, *Determination of the elements V_{us} and V_{ud} of the Kobayashi-Maskawa matrix*, *Z. Phys.* **C25** (1984) 91.

[61] P. Post and K. Schilcher, *K_{l3} form factors at order p^6 in chiral perturbation theory*, *Eur. Phys. J.* **C25** (2002) 427–443, [hep-ph/0112352].

[62] A. Duncan, E. Eichten and H. Thacker, *Electromagnetic splittings and light quark masses in lattice QCD*, *Phys. Rev. Lett.* **76** (1996) 3894–3897, [hep-lat/9602005].

[63] [MILC 08] S. Basak et al., *Electromagnetic splittings of hadrons from improved staggered quarks in full QCD*, *PoS* **LAT2008** (2008) 127, [0812.4486].

[64] T. Blum et al., *Electromagnetic mass splittings of the low lying hadrons and quark masses from 2+1 flavor lattice QCD+QED*, *Phys. Rev.* **D82** (2010) 094508, [1006.1311].

[65] [BMW 10C] A. Portelli et al., *Electromagnetic corrections to light hadron masses*, *PoS* **LAT2010** (2010) 121, [1011.4189].

[66] [MILC 04] C. Aubin et al., *Light pseudoscalar decay constants, quark masses and low energy constants from three-flavor lattice QCD*, *Phys. Rev.* **D70** (2004) 114501, [hep-lat/0407028].

[67] [ETM 14E] N. Carrasco, P. Dimopoulos, R. Frezzotti, P. Lami, V. Lubicz et al., *Leptonic decay constants f_K, f_D and f_{D_s} with $N_f = 2+1+1$ twisted-mass lattice QCD*, *Phys.Rev.* **D91** (2015) 054507, [1411.7908].

[68] [FNAL/MILC 14A] A. Bazavov et al., *Charmed and light pseudoscalar meson decay constants from four-flavor lattice QCD with physical light quarks*, *Phys.Rev.* **D90** (2014) 074509, [1407.3772].

[69] [ETM 13F] P. Dimopoulos, R. Frezzotti, P. Lami, V. Lubicz, E. Picca et al., *Pseudoscalar decay constants f_K/f_π, f_D and f_{D_s} with $N_f = 2+1+1$ ETMC configurations*, *PoS* **LATTICE2013** (2014) 314, [1311.3080].

[70] [HPQCD 13A] R. Dowdall, C. Davies, G. Lepage and C. McNeile, *V_{us} from π and K decay constants in full lattice QCD with physical u, d, s and c quarks*, *Phys.Rev.* **D88** (2013) 074504, [1303.1670].

[71] [MILC 13A] A. Bazavov, C. Bernard, C. DeTar, J. Foley, W. Freeman et al., *Leptonic decay-constant ratio f_{K^+}/f_{π^+} from lattice QCD with physical light quarks*, *Phys.Rev.Lett.* **110** (2013) 172003, [1301.5855].

[72] [MILC 11] A. Bazavov et al., *Properties of light pseudoscalars from lattice QCD with HISQ ensembles*, *PoS* **LAT2011** (2011) 107, [1111.4314].

[73] [ETM 10E] F. Farchioni, G. Herdoiza, K. Jansen, M. Petschlies, C. Urbach et al., *Pseudoscalar decay constants from $N_f = 2+1+1$ twisted mass lattice QCD*, *PoS* **LAT2010** (2010) 128, [1012.0200].

[74] [BMW 16] S. Dürr et al., *Leptonic decay-constant ratio f_K/f_π from lattice QCD using 2+1 clover-improved fermion flavors with 2-HEX smearing*, 1601.05998.

[75] E. E. Scholz and S. Dürr, *Leptonic decay-constant ratio f_K/f_π from clover-improved $N_f = 2+1$ QCD*, 2016. 1610.00932.

[76] [RBC/UKQCD 14B] T. Blum et al., *Domain wall QCD with physical quark masses*, *Phys. Rev.* **D93** (2016) 074505, [1411.7017].

[77] [RBC/UKQCD 12] R. Arthur et al., *Domain wall QCD with near-physical pions*, *Phys.Rev.* **D87** (2013) 094514, [1208.4412].

[78] J. Laiho and R. S. Van de Water, *Pseudoscalar decay constants, light-quark masses and B_K from mixed-action lattice QCD*, *PoS* **LATTICE2011** (2011) 293, [1112.4861].

[79] [MILC 10] A. Bazavov et al., *Results for light pseudoscalar mesons*, *PoS* **LAT2010** (2010) 074, [1012.0868].

[80] [JLQCD/TWQCD 10] J. Noaki et al., *Chiral properties of light mesons in $N_f = 2 + 1$ overlap QCD*, *PoS* **LAT2010** (2010) 117.

[81] [RBC/UKQCD 10A] Y. Aoki et al., *Continuum limit physics from 2+1 flavor domain wall QCD*, *Phys.Rev.* **D83** (2011) 074508, [1011.0892].

[82] [PACS-CS 09] S. Aoki et al., *Physical point simulation in 2+1 flavor lattice QCD*, *Phys. Rev.* **D81** (2010) 074503, [0911.2561].

[83] [BMW 10] S. Dürr, Z. Fodor, C. Hoelbling, S. Katz, S. Krieg et al., *The ratio F_K/F_π in QCD*, *Phys.Rev.* **D81** (2010) 054507, [1001.4692].

[84] [JLQCD/TWQCD 09A] J. Noaki et al., *Chiral properties of light mesons with $N_f = 2 + 1$ overlap fermions*, *PoS* **LAT2009** (2009) 096, [0910.5532].

[85] [MILC 09A] A. Bazavov et al., *MILC results for light pseudoscalars*, *PoS* **CD09** (2009) 007, [0910.2966].

[86] [MILC 09] A. Bazavov et al., *Full nonperturbative QCD simulations with 2+1 flavors of improved staggered quarks*, *Rev. Mod. Phys.* **82** (2010) 1349–1417, [0903.3598].

[87] C. Aubin, J. Laiho and R. S. Van de Water, *Light pseudoscalar meson masses and decay constants from mixed action lattice QCD*, *PoS* **LAT2008** (2008) 105, [0810.4328].

[88] [PACS-CS 08A] Y. Kuramashi, *PACS-CS results for 2+1 flavor lattice QCD simulation on and off the physical point*, *PoS* **LAT2008** (2008) 018, [0811.2630].

[89] [RBC/UKQCD 08] C. Allton et al., *Physical results from 2+1 flavor domain wall QCD and SU(2) chiral perturbation theory*, *Phys. Rev.* **D78** (2008) 114509, [0804.0473].

[90] [HPQCD/UKQCD 07] E. Follana, C. T. H. Davies, G. P. Lepage and J. Shigemitsu, *High precision determination of the π, K, D and D_s decay constants from lattice QCD*, *Phys. Rev. Lett.* **100** (2008) 062002, [0706.1726].

[91] [NPLQCD 06] S. R. Beane, P. F. Bedaque, K. Orginos and M. J. Savage, *f_K/f_π in full QCD with domain wall valence quarks*, *Phys. Rev.* **D75** (2007) 094501, [hep-lat/0606023].

[92] [ETM 14D] A. Abdel-Rehim, C. Alexandrou, P. Dimopoulos, R. Frezzotti, K. Jansen et al., *Progress in Simulations with Twisted Mass Fermions at the Physical Point*, *PoS* **LATTICE2014** (2014) 119, [1411.6842].

[93] [ALPHA 13A] S. Lottini, *Chiral behaviour of the pion decay constant in $N_f = 2$ QCD*, *PoS* **LATTICE2013** (2013) 315, [1311.3081].

[94] [BGR 11] G. P. Engel, C. Lang, M. Limmer, D. Mohler and A. Schäfer, *QCD with two light dynamical chirally improved quarks: mesons*, *Phys.Rev.* **D85** (2012) 034508, [1112.1601].

[95] [ETM 09] B. Blossier et al., *Pseudoscalar decay constants of kaon and D-mesons from $N_f = 2$ twisted mass lattice QCD*, *JHEP* **0907** (2009) 043, [0904.0954].

[96] [QCDSF/UKQCD 07] G. Schierholz *et al., Probing the chiral limit with clover fermions I: the meson sector, talk given at Lattice 2007, Regensburg, Germany*, PoS **LAT2007**, 133.

[97] D. Guadagnoli, F. Mescia and S. Simula, *Lattice study of semileptonic form-factors with twisted boundary conditions*, *Phys.Rev.* **D73** (2006) 114504, [hep-lat/0512020].

[98] [UKQCD 07] P. A. Boyle, J. Flynn, A. Jüttner, C. Sachrajda and J. Zanotti, *Hadronic form factors in lattice QCD at small and vanishing momentum transfer*, *JHEP* **0705** (2007) 016, [hep-lat/0703005].

[99] [SPQcdR 04] D. Bećirević et al., *The $K \to \pi$ vector form factor at zero momentum transfer on the lattice*, *Nucl. Phys.* **B705** (2005) 339–362, [hep-ph/0403217].

[100] G. Amoros, J. Bijnens and P. Talavera, *QCD isospin breaking in meson masses, decay constants and quark mass ratios*, *Nucl. Phys.* **B602** (2001) 87–108, [hep-ph/0101127].

[101] M. Lüscher, *Properties and uses of the Wilson flow in lattice QCD*, *JHEP* **08** (2010) 071, [1006.4518].

[102] [BMW 12A] S. Borsanyi, S. Dürr, Z. Fodor, C. Hoelbling, S. D. Katz et al., *High-precision scale setting in lattice QCD*, *JHEP* **1209** (2012) 010, [1203.4469].

[103] V. Cirigliano and H. Neufeld, *A note on isospin violation in $P_{\ell 2}(\gamma)$ decays*, *Phys.Lett.* **B700** (2011) 7–10, [1102.0563].

[104] [FLAG 10] G. Colangelo, S. Dürr, A. Jüttner, L. Lellouch, H. Leutwyler et al., *Review of lattice results concerning low energy particle physics*, *Eur.Phys.J.* **C71** (2011) 1695, [1011.4408].

[105] J. C. Hardy and I. S. Towner, *Superallowed $0^+ \to 0^+$ nuclear β decays: A new survey with precision tests of the conserved vector current hypothesis and the Standard Model*, *Phys. Rev.* **C79** (2009) 055502, [0812.1202].

[106] [JLQCD 15C] B. Fahy, G. Cossu, S. Hashimoto, T. Kaneko, J. Noaki and M. Tomii, *Decay constants and spectroscopy of mesons in lattice QCD using domain-wall fermions*, *PoS* **LATTICE2015** (2016) 074, [1512.08599].

[107] [TWQCD 11] T.-W. Chiu, T.-H. Hsieh and Y.-Y. Mao, *Pseudoscalar meson in two flavors QCD with the optimal domain-wall fermion*, *Phys.Lett.* **B717** (2012) 420–424, [1109.3675].

[108] [JLQCD/TWQCD 08A] J. Noaki et al., *Convergence of the chiral expansion in two-flavor lattice QCD*, *Phys. Rev. Lett.* **101** (2008) 202004, [0806.0894].

[109] [HPQCD 09B] C. T. H. Davies, E. Follana, I. Kendall, G. P. Lepage and C. McNeile, *Precise determination of the lattice spacing in full lattice QCD*, *Phys.Rev.* **D81** (2010) 034506, [0910.1229].